CHAPTER III

PHOTOEMISSION CALCULATIONS USING THE FREE ELECTRON MODEL

Photoelectric effect is of fundamental importance in physics as it is connected with the basic interaction of the electromagnetic field with the solid. Much of the current qualitative understanding of the bulk effects on photoemission is based on the free - electron (FE) model of the semi-infinite metal. In this simplest model, the surface barrier confining the electrons in the metal is represented by a step-function discontinuity in the potential. FE model has been applied in the theory of photoemission by Fowler[38], Mitchell[39] and others[5,10,40]. All these authors considered photoemission from free electron metals as an example of a pure surface effect.

In bulk photoemission, the necessary momentum is provided by the lattice and the surface induces the surface photoeffect as the incident photon carries too little momentum to be able to photoexcite electrons. The perpendicular component of the electromagnetic field undergoes a rapid spatial variation in the surface region of a metal and this is the main factor responsible for the cause of the surface photoemission. We will discuss here the photoemission from the free electron metals focusing mainly on aluminium.

The first unambiguous experimental evidence was contributions to the surface plasmon excitations due to surface roughness as seen by Endriz and Spicer[41]. Thereafter Flodström and Endriz[42] measured the ratio between the yields for p- and s-polarised light from aluminium at 5.4 eV and it could not be explained under the ordinary volume model of photoemission. Perhaps Feibelman[13] is the first one to calculate theoretically the photoyield treating the initial and final state wavefunctions as well as the electromagnetic field in the matrix element. He calculated the photoyield for photon energy below and above the plasmon energy for aluminium. Petersen and Hagstrom[9] were the first to obtain the absolute surface photoyield spectrum of aluminium by fully exploiting the properties of the synchrotron radiation. Then Levinson, Plummer and Feibelman[14] measured and calculated the normal cross-section for the surface state and the Fermi level of aluminium (100). The photoexcitation matrix element was calculated using the Lang-Kohn potential for the initial and final states as well as the dielectric response of the solid.

We shall calculate the photoemission cross-section from aluminium by using the golden rule formula (1.2), for which it is necessary to calculate $\langle \psi_f | H' | \psi_i \rangle$. We shall consider p-polarised radiation in the long wavelength limit, and we shall consider the z-component of $\vec{A}$ only. The relevant

expressions for the field are given by Bagchi and Kar[21]. The perturbation H′ due to the incident photon radiation in one dimension is given by

$$H' = \frac{e}{mc}\left[\tilde{A}_{\omega}(z)\,\frac{d}{dz} + \frac{1}{2}\,\frac{d}{dz}\,\tilde{A}_{\omega}(z)\right] \tag{3.1}$$

Photemission cross-section (PEC) was calculated by using the formula which may be derived from Eq. (1.2)[21]

$$\frac{d\sigma}{d\Omega} = \frac{k^2}{\omega}\,|\langle\psi_f|\tilde{A}_{\omega}(z)\,\frac{d}{dz} + \frac{1}{2}\,\frac{d}{dz}\,\tilde{A}_{\omega}(z)|\psi_i\rangle|^2 \tag{3.2}$$

To evaluate PEC in Eq. (3.2), we also need the initial state wavefunction ψ_i and the final state wavefunction ψ_f. Both ψ_i and ψ_f are calculated in the free electron approximation assuming a step like potential to be existing at the surface described by

$$V(z) = -V_o\theta(z) \tag{3.3}$$

which is shown in Fig. (3.1). In Eq. (3.3), we have $V_o=E_F+\phi$ where E_F is the Fermi level in the free electron model and ϕ is the work function. $\theta(z)$ is the step function described as

$$\theta(z) = \begin{cases} 0, & z<0 \\ 1, & z>0 \end{cases} \tag{3.4}$$

We have assumed the initial state wavefunction as

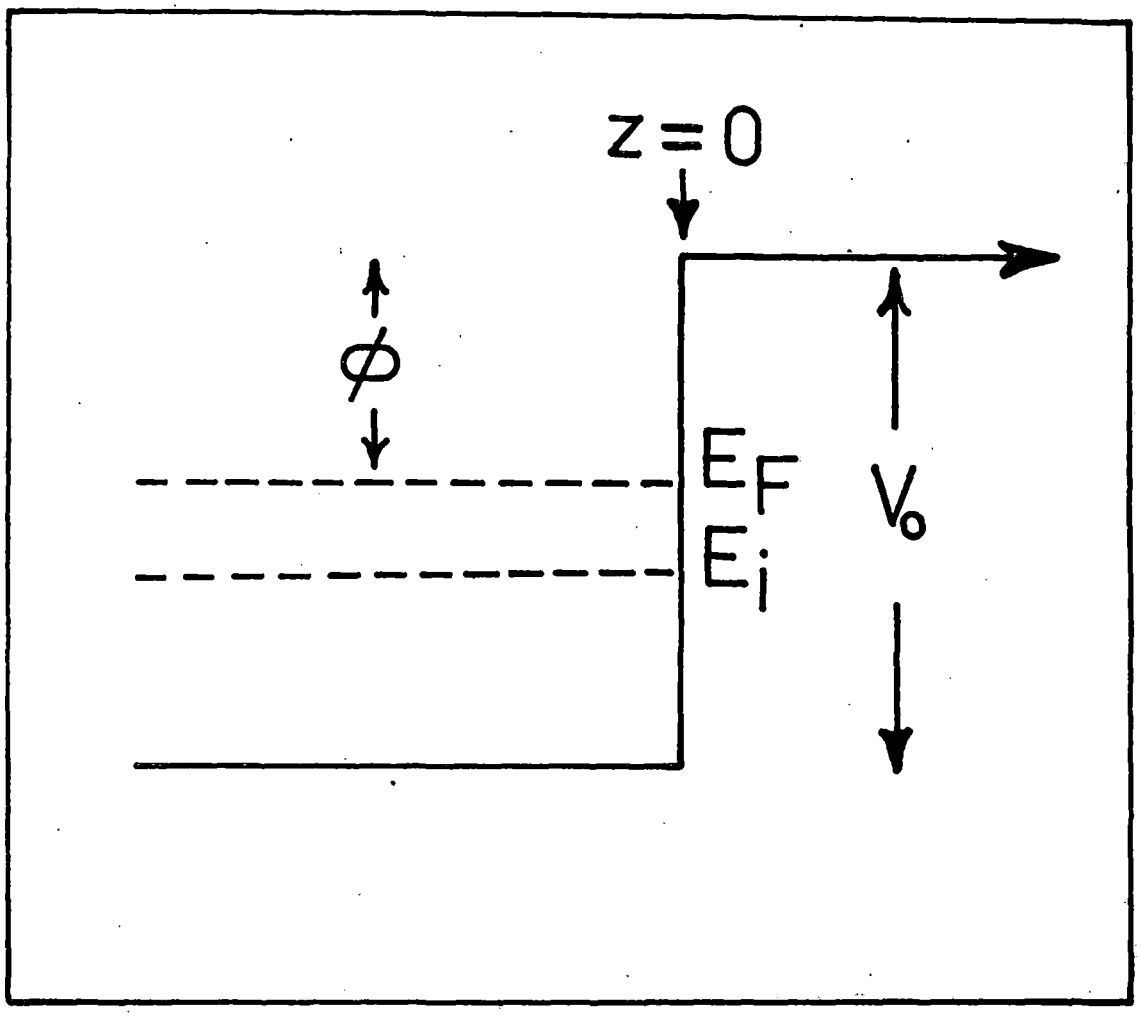

Figure 3.1

$$\psi_i(z) = \begin{cases} \sum A\, e^{i\vec{k}_{\parallel}\cdot\vec{r}_{\parallel}} \cdot (e^{ik_i z} + R\, e^{-ik_i z}), & z<0 \\ \sum A\, e^{i\vec{k}_{\parallel}\cdot\vec{r}_{\parallel}} \cdot T \cdot e^{-\varkappa z}, & z>0 \end{cases} \tag{3.5}$$

where A can be determined from the current normalisation and it turns out that $A = (m/2\pi\hbar^2 k_i)^{1/2}$.

Neglecting the transverse parts in Eq. (3.5), we can now write the initial state wavefunction as

$$\psi_i(z) = \begin{cases} \sum A\, (e^{ik_i} + R\, e^{-ik_i z}), & z<0 \\ \sum A\, T\, e^{-\varkappa z}, & z>0 \end{cases} \tag{3.6}$$

At z=0, the wavefunctions for the two regions can be written as

$$\psi_i(z)\Big|_{z\to 0^-} = A(1 + R)$$

$$\psi_i(z)\Big|_{z\to 0^+} = A\, T \tag{3.7}$$

The condition $\psi_i(z)\Big|_{z\to 0^-} = \psi_i(z)\Big|_{z\to 0^+}$ at the surface gives

$$1 + R = T \tag{3.8}$$

Now taking the derivatives of the initial state wavefunctions in the two regions, we have

$$\psi_i'(z) = Aik_i(e^{ik_i z} - R\, e^{-ik_i z}) \qquad \text{for } z < 0$$

$$\psi_i'(z) = -A\varkappa T\, e^{-\varkappa z}. \qquad \text{for } z > 0$$

At the surface(z=0), we have

$$\psi_i'(z)\Big|_{z\to 0^-} = Aik_i(1 - R)$$

and $$\psi_i'(z)\Big|_{z\to 0^+} = -A\varkappa T \quad .$$

But at the surface, using the condition

$$\psi_i'(z)\Big|_{z\to 0^-} = \psi'_i(z)\Big|_{z\to 0^+}$$

gives $$ik_i(1 - R) = -T \; . \qquad (3.9)$$

Solving Eqs. (3.8) and (3.9), we get

$$R = \frac{ik_i + \varkappa}{ik_i - \varkappa}$$

$$T = \frac{2ik_i}{ik_i - \varkappa} \qquad (3.10)$$

Putting the values of R and T from Eq. (3.10) in Eq. (3.6), we can write the initial state wavefunction for the free electron model as, following Bagchi and Kar[21]

$$\psi_i(z) = \begin{cases} \left(\frac{m}{2\pi\hbar^2 k_i}\right)^{1/2} \left[e^{ik_i z} + \frac{ik_i + \varkappa}{ik_i - \varkappa} e^{-ik_i z} \right] . e^{i\vec{k}_\parallel . \vec{r}_\parallel} , & z<0 \\ \left(\frac{m}{2\pi\hbar^2 k_i}\right)^{1/2} \frac{2ik_i}{ik_i - \varkappa} e^{-\varkappa z} . e^{i\vec{k}_\parallel . \vec{r}_\parallel} , & z>0 \end{cases} \tag{3.11}$$

where the parameters are described as follows:

$$k_i^2 = \frac{2mE_i}{\hbar^2} - \vec{k}_\parallel^2$$

$$\varkappa^2 = \frac{2m}{\hbar^2} (V_o - E_i) + \vec{k}_\parallel^2 . \tag{3.12}$$

$\vec{k}_\parallel$ and $\vec{r}_\parallel$ are the component of $\vec{k}$ and $\vec{r}$ in the x-y plane which is parallel to the surface. The final state wavefunction is the scattering state of the step potential V(z). This may be written as, following Bagchi and Kar [21]

$$\psi_f(z) = \begin{cases} \left(\frac{m}{2\pi\hbar^2 q}\right)^{1/2} \frac{2q}{q + k_f} e^{-\alpha|z|} e^{ik_f z} . e^{i\vec{k}_\parallel . \vec{r}_\parallel} , & z<0 \\ \left(\frac{m}{2\pi\hbar^2 q}\right)^{1/2} \left[e^{iqz} + \frac{q - k_f}{q + k_f} e^{-iqz} \right] e^{i\vec{k}_\parallel . \vec{r}_\parallel} , & z>0 \end{cases} \tag{3.13}$$

where $$k_f^2 = \frac{2m}{\hbar^2} E_f - k_{\parallel}^2$$

$$q^2 = \frac{2m}{\hbar^2} (E_f - V_o) - k_{\parallel}^2 \qquad (3.14)$$

and $E_f = E_i + \hbar\omega$. The matrix element for photoemission cross-section in Eq. (3.2) was evaluated by using the above expressions for the wavefunctions and the vector potential of Eq. (2.3). To ensure convergence of the integral for $z<0$, a convergence factor α was introduced which arises due to lifetime effects[12]. This is a standard procedure in low energy electron diffraction and photoemission calculations. We do it by introducing a factor $e^{-\alpha|z|}$ in the calculation of the matrix element for the region $z<0$. This is done to take into account the inelastic scattering of the electrons.

For surface state photoemission calculations, the initial state wavefunction ψ_i is replaced by a properly normalised Gaussian wavefunction as used by Bagchi and Kar[21] which is given by

$$\psi_i(z) = e^{i\vec{k}_{\parallel}\cdot\vec{r}_{\parallel}} \left(\frac{2\beta}{\pi a^2} \right)^{1/4} . e^{-\beta(z-z_o/a)^2} \qquad (3.15)$$

where β is a dimensionless parameter that describes the width of the Gaussian so that its full width at half maximum is given

by $\Delta=2a/\beta$. In Eq. (3.15), $\psi_i(z)$ is centred on the $z=z_o$ plane. The calculation of the photoemission cross-section for normal photoemission now reduces to the evaluation of the matrix element $\langle\psi_f|H'|\psi_i\rangle$. Rewriting Eq. (3.2), we have the formula for calculating the photoemission cross-section given by

$$\frac{d\sigma}{d\Omega} = \frac{k^2}{\omega}|I|^2 \tag{3.16}$$

where I is given by

$$\begin{aligned} I &= \int_{-\infty}^{\infty} \psi_f^*(z)\, H'\psi_i(z)dz \\ &= \int_{-\infty}^{-a/2} \psi_f^*\, \tilde{A}_\omega(z)\, \frac{d\psi_i}{dz}\, dz \;+\; \int_{-a/2}^{0} \psi_f^*\, \tilde{A}_\omega(z)\, \frac{d\psi_i}{dz}\, dz \\ &\quad + \frac{1}{2}\int_{-a/2}^{0} \psi_f^*\, \frac{d\tilde{A}_\omega(z)}{dz}\, \psi_i dz \;+\; \int_{0}^{a/2} \psi_f^*\, \tilde{A}_\omega(z)\, \frac{d\psi_i}{dz}\, dz \\ &\quad + \frac{1}{2}\int_{0}^{a/2} \psi_f^*\, \frac{d\tilde{A}_\omega(z)}{dz}\, \psi_i dz \;+\; \int_{a/2}^{\infty} \psi_f^*\, \tilde{A}_\omega(z)\, \frac{d\psi_i}{dz}\, dz \end{aligned} \tag{3.17}$$

Photoemission cross-section (PEC) was calculated from the band state (Fermi level) and surface state. The detailed evaluation

of the integral in Eq. (3.17) is shown in appendix I. The fortran program used for the numerical evaluation of integral I is given in appendix III. We have applied our results for calculating the normal photoemission from the Fermi level of aluminium for which the experimental data as well as the theoretical calculations using the jellium model is available. The data used are, as given by Ashcroft and Mermin[43], for work function ϕ=4.25 eV and initial state energy E_i=11.7 eV. Since the normal photoemission is considered, $\vec{k}_{\parallel}$=0 and θ_i is taken to be 45^{o} as in the experiment. The PEC results with a=10 a.u and α=0.35 is shown in Fig. (3.2). The calculated photocurrent results shows a peak at 11 eV, minimum at 15 eV and again a broad peak at 20.5 eV.

The origin of peak at 11 eV in the calculated spectrum was further investigated as shown in Fig. (3.3). Here $|\tilde{A}_{\omega}(z)|$ was plotted as a function of z in the surface region for photon energy at 20 eV, 11 eV and 15 eV respectively. It is seen that a strong peak occurs at 11 eV in the middle of the surface but at 15 eV and 20 eV, the plot does not show any peak in the surface region. As a further evidence of peak at 11 eV being surface related, we have also done calculations of photocurrent using free electron wavefunctions as in Eqs. (3.11) and (3.13) with fields as given by Fresnel refraction formula[44]. The plot shows a minimum at 12 eV and no peak at 11-12 eV. Above the

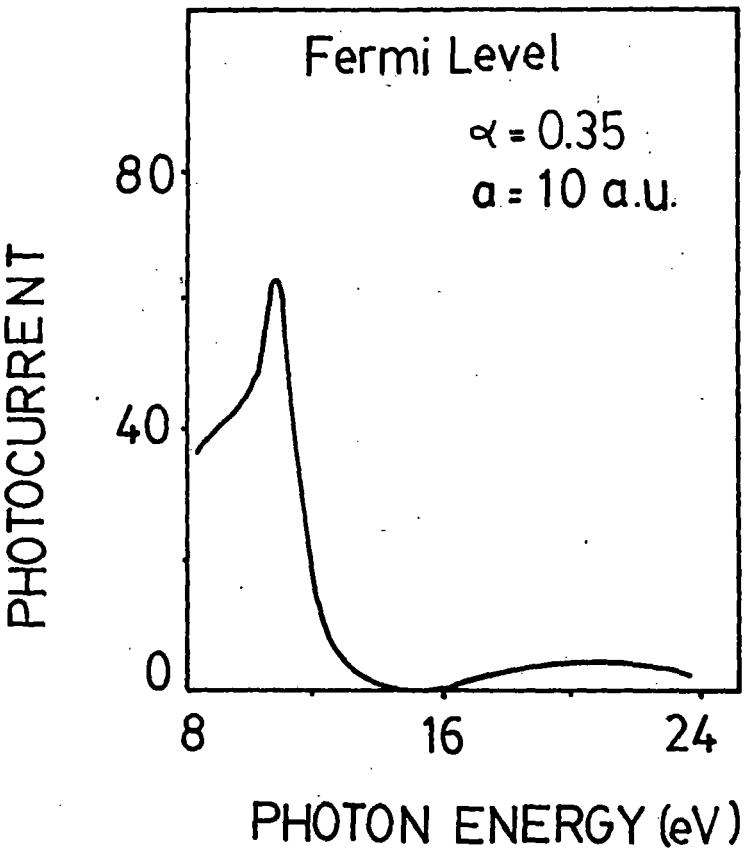
Fermi Level
α = 0.35
a = 10 a.u.
80
40
0
PHOTOCURRENT
8
16
24
PHOTON ENERGY (eV)

Figure 3.2

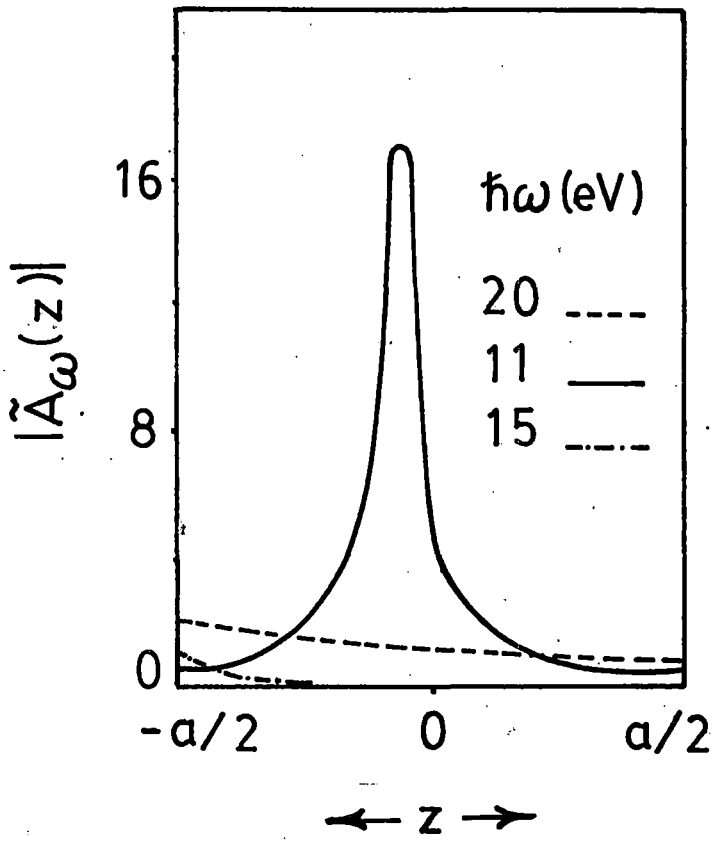

Figure 3.3

plasmon energy, the plot shows a peak (Fig. 3.4) which is more pronounced then that with the surface region included. Thus it is evident that the simple Fresnel refraction formula is inadequate in reproducing the surface photoemissive features and the inclusion of the surface in photoemission calculations is important.

The results of the surface state photoemission is shown in Fig. (3.5) for aluminium. We have considered the surface state energy to lie at 2.75 eV below the Fermi level[14]. The photocurrent is calculated for the surface widths 5 a.u and 10 a.u. The height of photocurrent peak is greater for the narrow surface width than the broad one. Also the calculated data showed a qualitative agreement with the experimental data of Levinson et al[14].

We find therefore that the frequency dependence of normal component of the electric field near the surface of metal has important consequences for the angle resolved photoemission from the bulk as well as from the surface of aluminium. The field component in the surface region decreases greatly near the plasma frequency and these features explains the observed decrease in normal photoemission from the metallic surface states near plasmon energy. We therefore conclude that the inclusion of refraction effects is essential in a complete angle resolved photoemission calculations.

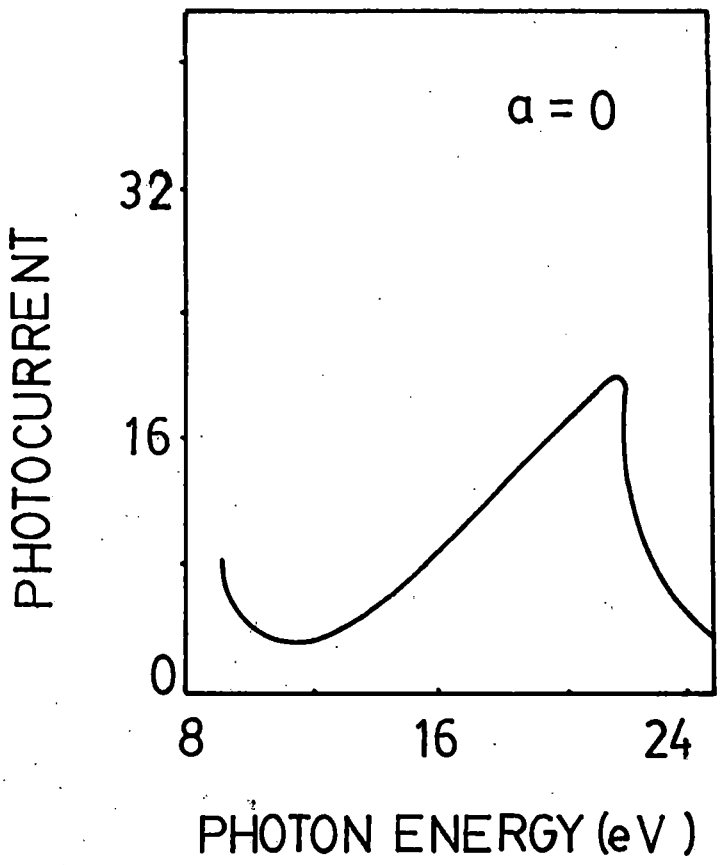

Figure 3.4

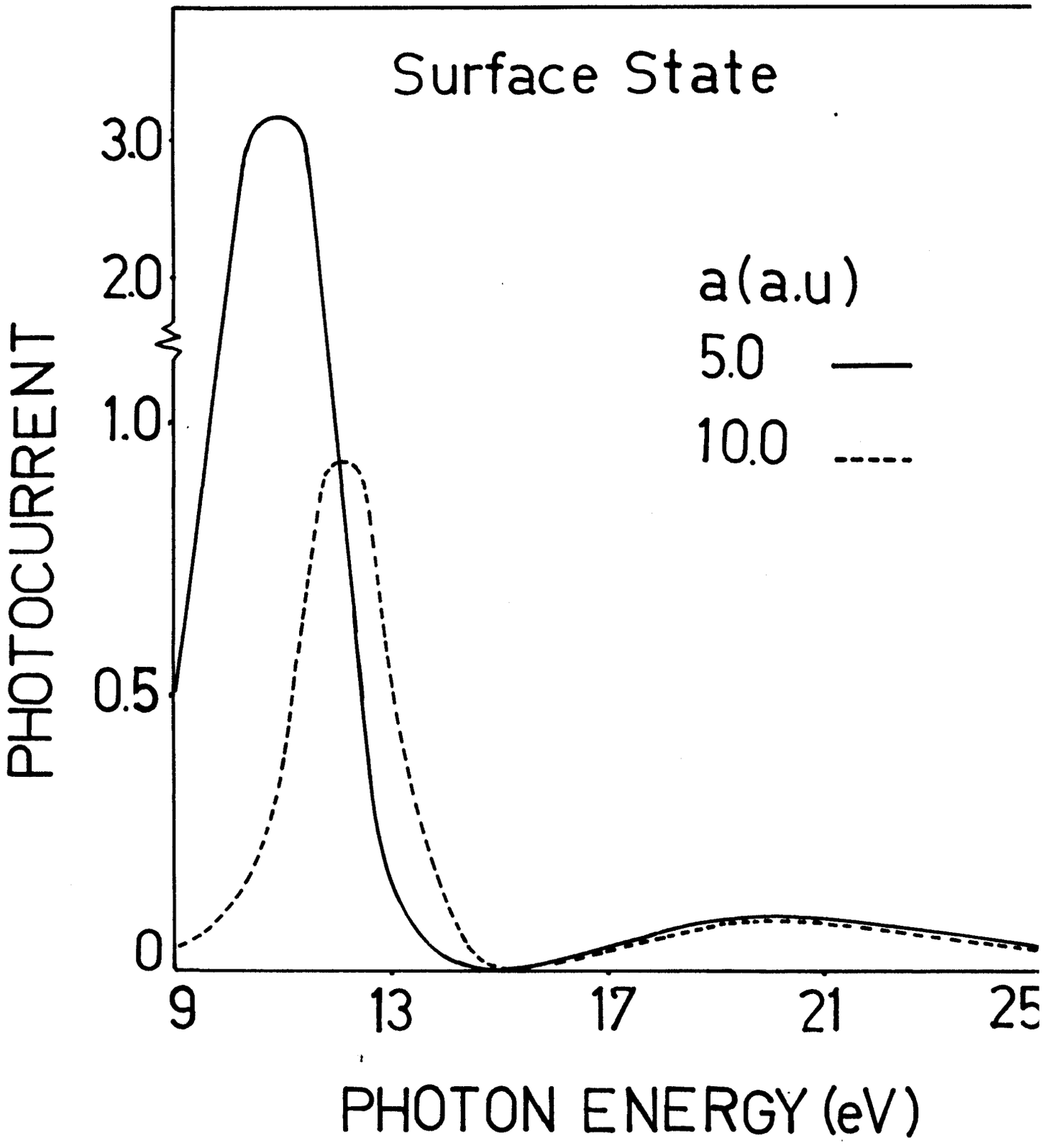
Surface State
3.0
2.0
1.0
0.5
0
PHOTOCURRENT
a(a.u)
5.0
10.0
9
13
17
21
25
PHOTON ENERGY (eV)

Figure 3.5